

The effect of composite-elastomer isolation system on the seismic response of liquid-storage tanks: Part I

A. Shahrjerdi^{*1} and M. Bayat^{2a}

¹Department of Mechanical Engineering, Malayer University, Malayer, Iran

²Department of Civil Engineering, Aalborg University, Denmark

(Received February 3, 2018, Revised July 10, 2018, Accepted September 11, 2018)

Abstract. A typical viable technique to decrease the seismic response of liquid storage tanks is to isolate them at the base. Base-isolation systems are an efficient and feasible solution to reduce the vulnerability of structures in high seismic risk zones. Nevertheless, when liquid storage tanks are under long-period shaking, the base-isolation systems could have different impacts. These kinds of earthquakes can damage the tanks readily. Hence, the seismic behaviour and vibration of cylindrical liquid storage tanks, subjected to earthquakes, is of paramount importance, and it is investigated in this paper. The Finite Element Method is used to evaluate seismic response in addition to the reduction of excessive liquid sloshing in the tank when subjected to the long-period ground motion. The non-linear stress-strain behaviour pertaining to polymers and rubbers is implemented while non-linear contact elements are employed to describe the 3-D surface-to-surface contact. Therefore, Nonlinear Procedures are used to investigate the fluid-structure interactions (FSI) between liquid and the tank wall while there is incompressible liquid. Part I, examines the effect of the flexibility of the isolation system and the tank aspect ratio (height to radius) on the tank wall radial displacements of the tank wall and the liquid sloshing heights. Maximum stress and base shear force for various aspect ratios and different base-isolators, which are subjected to three seismic conditions, will be discussed in Part II. It is shown that the composite-base isolator is much more effective than other isolators due to its high flexibility and strength combined. Moreover, the base isolators may decrease the maximum level pertaining to radial displacement.

Keywords: base isolation; liquid storage tank; earthquake; composite-elastomeric; seismic response

1. Introduction

Some storage tanks have been placed in high seismic hazard zones where the focus on their behavior can be considerable. For instance, a fixed roof steel storage tank with more than 500,000 crude oil barrels' capacity may be located in high risk zone (Fig. 1(c)). Fuel storage regions are especially defenseless sub-systems of industrial plants deciding for the relevant risk, hence the classification of oil storage tanks as hazard. Since many industrial facilities in Iran are often located in earthquake-prone zones, it can be noted that any failure in storage tank functioning, such as hazardous waste, air pollution, flammable and combustible fluid, or damage taken due to explosion, can have direct and indirect effects on safety.

The behavior of liquid-storage tanks during earthquakes is very momentous, far beyond the mere economic value of the tanks and contents. If, for instance, a water tank collapses, as it did during the 1990 Manjil-Rudbar, Gilan, Iran earthquake, the loss of the public water supply can have serious consequences. Similarly, the failure of tanks storing combustible materials, such as gasoline and other

petroleum products, may lead to extensive, uncontrolled fires, as it did during the 1978 Tabas, Iran, earthquake. Liquid storage tanks have complicated seismic behavior due to fluid-structure interaction and variable liquid tank weight resulting from unsteady liquid free surface (Shekari *et al.* 2010). There have been several reports on damage in liquid storage tanks in past earthquakes (Steinbrugge and Flores 1963, Hanson 1973, Jennings and Housner 1973, Manos 1986, Hall *et al.* 1994). Seismic events caused considerable damages to liquid storage tanks recently. Buckling and failure in tank roof are the most commonplace damage in the tank walls due to compressive stress and liquid surface pressure (Niwa and Clough 1982, Manos and Clough 1985, Manos and Talaslidis 1988).

The most commonly used analytical model for estimating the dynamic response of liquid containers was developed by Housner (1963). In this model, the hydrodynamic pressure induced by seismic excitations was separated into impulsive and convective components using lumped mass approximation. The famous Housner method enabled engineers to conduct the seismic response analysis of lofty tanks using a two-mass idealization. The effect of wall flexibility on the hydrodynamic pressure distribution was studied by Yang (1976). A different approach to the solution of the problem of flexible containers was developed by Veletsos (1974). He presented a simple procedure for evaluating the hydrodynamic forces induced in flexible liquid-filled tanks. Later, Veletsos and Yang (1977) presented simplified formulas to obtain the

*Corresponding author, Assistant Professor

E-mail: Shahrjerdi@malayeru.ac.ir,
alishahrjerdi2000@yahoo.com

^aPh.D.

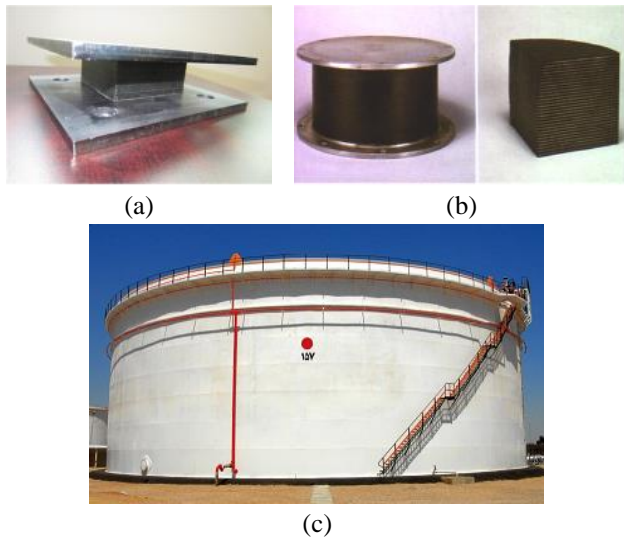


Fig. 1 (a) Fiber-Reinforced Elastomeric Isolators (FREI), (b) Steel-Base Rubber Bearings (SRB) (KAmrAvA 2015), (c) storage tank

fundamental natural frequencies of the liquid-filled shells by the Rayleigh-Ritz energy method. Nonlinear behavior of liquid sloshing of partially filled rectangular tank is studied by Goudarzi and Sabbagh-Yazdi (2012). Using viscous mass damper (VMD) with a rubber bearing to develop the hybrid control system and reduce the sloshing of cylindrical tanks underground motions is studied by Zhang *et al.* (2016) recently.

The base isolation method have been evolved and successfully applied to buildings in the past (Kelly 1986, Jangid and Datta 1995, Losanno *et al.* 2014, Chen *et al.* 2016). Sloshing response of a double deck type floating roof (DDFR) cylindrical liquid storage tank with the under seismic excitation is studied by Goudarzi (2015). Using extended Hamiltonian variational principle, the response of the floating roofed storage tanks is evaluated for different types of ground motions, including near-source and long-period far-field records by Golzar *et al.* (2012). Kim and Lee (1995) experimentally investigated the seismic performance of liquid storage tanks isolated by laminated rubber bearings under unidirectional excitation. Malhotra (1997) studied the seismic response of cylindrical liquid storage tanks, under unidirectional ground motion, in which the tank wall was isolated from the bottom plate by horizontal flexible rubber bearings. Wang *et al.* (2001) observed the seismic performance of liquid storage tank, isolated by friction pendulum system (FPS) under unidirectional excitation. Shrimali and Jangid (2002) investigated the response of liquid storage tanks isolated by the sliding bearings under bi-directional earthquake ground motions.

The efficiency of the Friction Pendulum System (FPS) for base isolation of liquid storage tanks was also investigated by Abali and Uckan (2010). The effects of overturning moment and vertical acceleration were considered in their study. Earthquake records with near-fault characteristics have long-period components that may affect the long-period sloshing motion of the liquid (Bagheri *et al.* 2005). Also, numerical methods like boundary element method

(BEM) and/or finite element method (FEM) have been utilized to investigate the effects of seismic base-isolation systems on the response of liquid storage tanks recently (Kim *et al.* 2002, Cho *et al.* 2004, Shekari *et al.* 2009).

Replacing steel with fiber, isolators of far less weight can be manufactured. Bearings with elastomeric damping material and fiber reinforcement are called fiber-reinforced elastomeric isolator (FREI) bearings. One of the advantages of Fiber-reinforced isolators is that they can be readily reshaped which is almost impossible with steel reinforced isolators. Another advantage of using fiber reinforcement is their stretchability under loading and their flexibility in bending. The steel reinforcement is supposed to be rigid and inextensible in bending. Fiber reinforcement with cords using individual fibers is studied by Kelly and Takhirov (2002). Tsai and Kelly (2002) studied the bending and compressive stiffness of fiber-reinforced isolators theoretically which have three kinds of geometry: infinitely long strip, circular and rectangular. Kelly and Takhirov (2001) conducted experiments on circular un-bonded fiber-reinforced bearings. The vertical pressure and the strain level were changed and the variations in damping as well as lateral stiffness were studied. Moon *et al.* (2002) made FREI bearings and carried out experiments under various loading conditions. They compared the performance of steel reinforced elastomeric isolators with the performance of the FREIs. Recently, an analytical seismic analysis with mathematical model was applied to finding the frequency response of elastic fluid-filled storage tanks by Giorgio *et al.* (2016), whose work was based on the use of high contrast multi-scale resonators to be compared by numerical simulation. The main results of their work focused on the response of the fuel tank in the frequency domain under a seismic excitation and the effect of the multi-scale resonators on the fluid sloshing waves in the transient domain.

So far little effort has been made to better understand the dynamic behavior of base-isolated liquid storage tanks under long-period ground motions. As a result, in this first part we have endeavored to accomplish this mission to get a good understanding of the dynamic response of base-isolated tanks; in the second paper, this understanding will be broadened, and the other aspects of dynamics behavior pertaining to base-isolated tanks will be set forth.

In this research, the dynamic behavior of various base-isolation systems for slender, medium, and broad tanks is studied while considering different ground motion records. The main objective of the present study is to investigate the effect of different parameters, such as the tank geometry aspect ratio (height to diameter), and the effect of composite isolators on the seismic response of liquid storage tanks when using both elastomer and fiber reinforced in base isolator as shown in Figs. 1(a)-1(b) (Yu *et al.* 2016).

In order to decrease the sloshing height of liquid, and decrease the failure of tanks, baffle is used. The Finite Element Analysis is implemented, and Fluid-Structure Interaction (FSI) is modeled by boundary elements and finite shell elements. Composite-elastomeric was employed for the base-isolation system. Finally, the impact of base-isolation systems on the seismic response of liquid storage tanks, which are subjected to different seismic ground

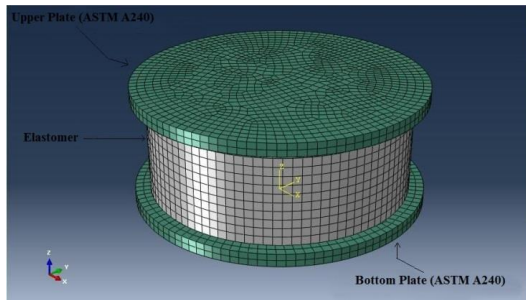


Fig. 2 Modelling of the isolator type I

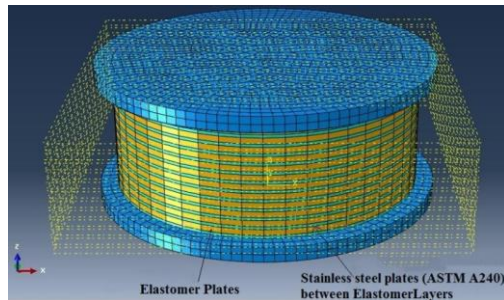


Fig. 3 Modelling of the isolator type II

motions by diverse predominant periods, is investigated. Using of composite elastomeric as a part of a base isolator has not been reported in the literature until now. The main results of this study may be that, composite base isolator can be reduced significantly sloshing and radial displacement due to flexibility and strength of carbon fiber and elastomer. Baffles also can be applied for sloshing height control.

The second paper will be devoted to the effect of base-isolation on base shear force and maximum stress of tanks wall, which are two major parameters in base-isolated liquid storage tanks design.

2. Isolators modelling

Isolators are tools that protect structures against earthquakes. Base-isolators are one of the applicable tools corresponding to seismic engineering to control the vibration of structures. In this section, using FE software, three different types of isolators have been described.

2.1 Isolator type I

The first type of isolators is consisting of two steel fixing plates located at the top and bottom of the bearing, which is a central lead core, and several alternating layers of elastomer, as shown in Fig. 2. Elastomer used in this isolator is made of Neoprene with hyper-elastic and visco-elastic properties which provide the isolation component with lateral flexibility; the lead core, which is used in all the three models, provides energy absorption (or damping), while the internal parts boost the vertical load capacity whilst minimizing bulging 33. The whole elements contribute to the lateral stiffness. The elastomer layers deform laterally during the structure seismic excitation

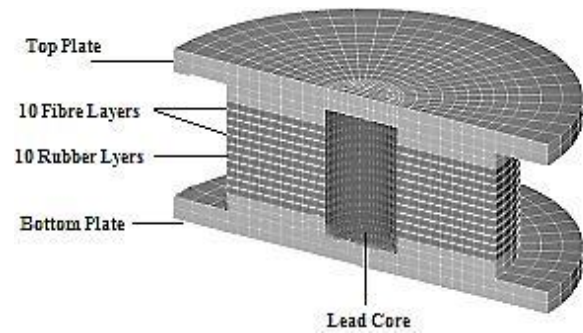


Fig. 4 The cutaway view of composite isolator (Andrade and Tuxworth 2009)

which allows the structure to move horizontally, and the bearing to absorb energy when the lead core yields.

2.2 Isolator type II

The second type of isolators is the elastomeric Lead-Plug Bearing (LPB), which is generally used for the base isolation of structures (Andrade and Tuxworth 2009) (Fig. 7). The isolator type II has a lead core just like the previous one, but, in addition, they have also reinforced elastomer with steel layers; therefore, in these types of isolators, we have diverse properties in comparison with the type I. The internal steel shims enhance the vertical load capacity whilst minimizing bulging (Andrade and Tuxworth 2009). The steel shims, along with the top and bottom steel fixing plates, also limit the plastic deformation of the central lead core. The overview of simulation of type II is shown in Fig. 3.

2.3 Isolator type III

The third types of investigated isolators contain fiber carbon isolators with orthotropic behavior which are used with elastomer together. Isolator fibers, as an instance of composite materials, are added to improve the mechanical properties of the elastomers (Fig. 4). Mechanical properties, such as tensile strength in polyurethane elastomers in terms of elongation to failure, are much higher than that of conventional elastomers (Andrade and Tuxworth 2009). Zhang *et al.* (2007) presented a new model which uses short fiber composites. In their study, polyurethane elastomer composites were prepared using milled fiberglass treated with coupling agent which can lead to the formation of satisfactory microstructures, and further increase tensile strength and hardness as well as the elongation percent of the composites. Although the powdery fillers increase the tensile strength, percent elongation at break point, which is a measure of flexibility, would be reduced (Das *et al.* 2012). The results show that short fibers are a good choice for making elastomer-composite isolators.

In composite isolator, due to the hyper-elastic and viscoplastic elastomer which is synchronized with the orthotropic properties of fiber, this isolator has complicated behavior in comparison to other isolators. Both isolators have a lead core in their center of elastomer that ties to the top and bottom plates, and is pressed in to the elastomer center hole.

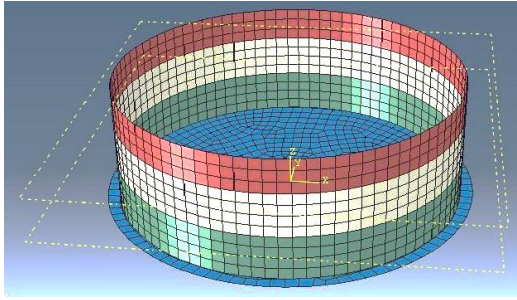


Fig. 5 An overview of the simulation of tank without separators

Composite-elastomer isolators are one of the newest methods for making huge isolators. The influence of these isolators on the seismic response of liquid storage tank is the goal of this study.

3. Finite element method

To analyze the seismic response of liquid storage tanks, The Finite-Element Method is used. A complete finite element simulation and analysis flow chart is reported for the sake of easy discussion, Fig. 8. The isolator was modeled using ABAQUS 6.13-4 (ABAQUS) Multi-physics finite-element software. Three types of isolators including elastomer, steel-elastomer, and composite elastomer were modeled and analyzed. Accordingly, the circular part of tank (bottom of the tank) is modeled; afterwards, the cylindrical part is created. In order to apply various thicknesses to the cylindrical part of it, the tank has been divided into several sections, in which each course has its own thickness. Fig. 5 shows a simulated tank with varying thickness for each course and without any separators.

In the next step, the other parts of the tank are assembled to it; then, the dynamic step is chosen to solve and analysis the problem.

4. Element types

Each layer of fiber-reinforcement in the composite-elastomer isolator was made up of thin layers of bidirectional (0/90 orientation) carbon fiber fabric. Inasmuch as elastomer (rubber) is almost incompressible material; the FE mesh with elements is designed, which allows for a hybrid formulation. The specimens are considered as 3D domains. Thus, the 8-node 3D solid elements with hybrid formulation C3D8H are used (Fig. 6). Three solid elements are used to model the elastomer between the fiber steel layers. The element has three translational degrees of freedom at each node along x , y , and z directions (Fig. 6). In order to keep the end plates relatively rigid, highly large elastic modulus was utilized. Lateral loading causes separation between the top surface of the isolator and the top plate as well as the bottom surface of the isolator and the bottom plate. Using disjointed models for the isolator and the endplates, the analysis would be erroneous as the transfer of load would not take place,

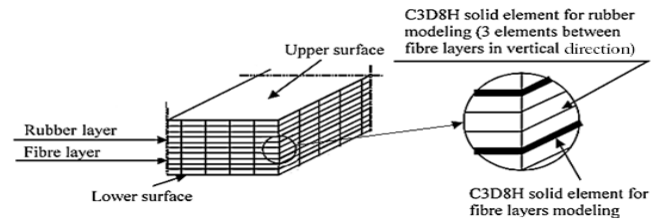


Fig. 6 Solid structural FE element for specimens

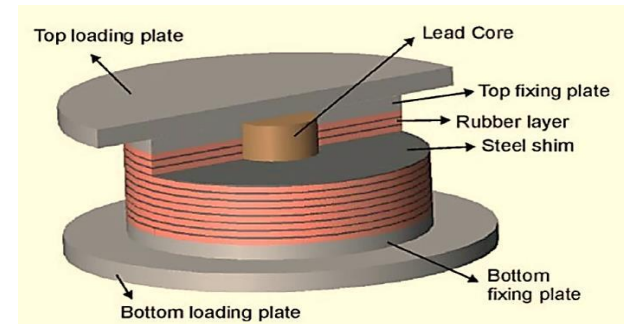


Fig. 7 Lead-Plug Bearings (LPB) isolator components (Andrade and Tuxworth 2009)

Table 1 Material properties of the tank (ASTM A36 Standard 2008)

ρ	Mass Density (Kg/m^3)	7800
E	Elastic Module (GPa)	208
ν	Poisson Ratio	0.3

and the elements would behave independently of each other. Hence, contact elements were introduced to model the isolator-plate interfaces. This modeling was done using 3-D surface-to-surface contact elements. Rough contact surface was utilized since the shear force should be transferred from the end plate to the isolator. Contact elements are non-linear, thus the difficulty of their solution.

5. Materials

Elastomer and Composite

The mechanical properties of the tank (based on ASTM A36 (Standard 2008)) in addition to the first, second, and third isolators are shown in Table 1 and Table 2. Fig. 7 shows the 3D overview of the isolators. Elastomer was modeled with hyperelastic and viscoelastic parameters.

Hyperelasticity is the ability to experience large elastic strain, which is recoverable. Rubber-like and many other polymer materials fall in this category. The strain energy potentials are used to obtain the constitutive behavior of the hyperelastic materials. Further, hyperelastic materials, generally, have very small compressibility. This is often referred to as incompressibility. Hyperelastic materials have a kind of stiffness that varies with the stress level. Ogden 3-terms model (Ogden 1972) was adopted to model the hyperelastic behavior of the rubber, and the viscoplastic behavior was modeled by Prony Viscoelastic Shear Response parameters, as shown in Table 2.

The matrix (1) is the stiffness matrix of the orthotropic

Table 2 Material properties of elastomer isolator, elastomer-Steel isolator, and elastomer-Composite isolator (Das *et al.* 2012)

Elastomer isolator					
Material		Mechanical properties			
Top, Bottom plate and Steel sheets	ASTM A240	E (GPa)	241		
		ν	0.32		
		ρ (kg/m ³)	7850		
		G (Pa)	450000		
		Hyper elastic	$\mu 1$	1890000	
			$\mu 2$	3600	
			$\mu 3$	-30000	
		Elastomer/ composite		$\alpha 1$	1.3
				$\alpha 2$	5
				$\alpha 3$	-2
$a 1$	0.3333				
$a 2$	0.3333				
$t 1$	0.4				
Visco elastic		$t 2$	0.2		
		Composite Orthotropic properties with carbon fiber shown in Table 3			
		E (Pa)	2.5E+11		
Core	Lead	ν	0.26		
		ρ (kg/m ³)	9100		

material, in which G is the shear modulus, $\mu 1, \mu 2, \mu 3, \alpha 1, \alpha 2$ and $\alpha 3$ are the Ogden 3-terms. The non-linear stress-strain behaviour of complex materials, such as polymers and rubbers, can be described by the Ogden material model (hyperelastic material model). This model was developed by Ray W. Ogden in 1972 (Soleimanloo and Barkhordari 2013). The Ogden model, as other hyperelastic material models, surmises that the material behaviour can be represented by means of a strain energy density function, from which the stress-strain relationships can be derived, $a 1, a 2, t 1$ and $t 2$ Prony Viscoelastic Shear Response parameters.

$$\begin{bmatrix} \frac{1 - \nu_{23}\nu_{32}}{E_2 E_3 \Delta} & 2.13 \times 10^{10} & \frac{\nu_{31} + \nu_{21}\nu_{32}}{E_2 E_3 \Delta} & 0 & 0 & 0 \\ \frac{\nu_{21} + \nu_{23}\nu_{31}}{E_2 E_3 \Delta} & 5.52 \times 10^{10} & \frac{\nu_{32} + \nu_{12}\nu_{31}}{E_1 E_3 \Delta} & 0 & 0 & 0 \\ \frac{\nu_{31} + \nu_{21}\nu_{32}}{E_2 E_3 \Delta} & \frac{\nu_{32} + \nu_{12}\nu_{31}}{E_1 E_3 \Delta} & \frac{1 - \nu_{12}\nu_{21}}{E_1 E_2 \Delta} & 0 & 0 & 0 \\ 0 & 0 & 0 & G_{23} & 0 & 0 \\ 0 & 0 & 0 & 0 & G_{31} & 0 \\ 0 & 0 & 0 & 0 & 0 & G_{12} \end{bmatrix} \quad (1)$$

In which

$$\Delta = \frac{(1 - \nu_{12}\nu_{21} - \nu_{23}\nu_{32} - \nu_{13}\nu_{31} - \nu_{21}\nu_{32}\nu_{13})}{E_1 E_2 E_3} \quad (2)$$

By substituting the modulus of elasticity, Poisson’s ratio, and shear modulus from Table 3 with the matrix (1), the matrix (3) will be obtained.

The matrix (3) has been derived from the stiffness matrix of orthotropic materials (1) that depend on the Young’s modulus, Poisson coefficient, and shear modulus in three directions.

Table 3 Mechanical properties of fiber reinforced for isolator type 3 (Das *et al.* 2012)

E_1	E_2	E_3	ν_{12}	ν_{23}	ν_{13}	G_{12}	G_{23}	G_{13}
4.4E+10	4.4E+10	1E+10	0.3	0.25	0.25	1E+10	5E+09	5E+09

Table 4 Dimensions of tanks of whole system

Tank No.	H (m)	D (m)	h (m)	Type
1	15	10	13.5	Slender
2	8	10	7	Medium
3	4	10	3	Broad

Table 5 Dimension of baffle for each tank

Type of tank	Slender	Medium	Broad
H_B	12	6.4	3.2
D_B	8	8	8

Table 6 Dimension of elastomer isolator

Diameter of elastomer (D_e)	900 mm
Total height (H_T)	300 mm
Thickness of Rubber (t_R)	260 mm
Top & Bottom plate Diameter (D_P)	1000 mm
Thickness of Top & Bottom (t_P)	20 mm
Diameter of Lead Core (D_c)	300 mm
Number of Rubber layer (n_R)	10
Thickness of Steel (t_S)	12 mm
Number of Steel layer (n_S)	10
Thickness of fiber (t_f)	12 mm
Number of fiber layer (n_f)	10

$$\begin{bmatrix} 5.52 \times 10^{10} & 2.13 \times 10^{10} & 1.91 \times 10^{10} & 0 & 0 & 0 \\ 2.13 \times 10^{10} & 5.52 \times 10^{10} & 1.91 \times 10^{10} & 0 & 0 & 0 \\ 1.91 \times 10^{10} & 1.91 \times 10^{10} & 1.22 \times 10^{10} & 0 & 0 & 0 \\ 0 & 0 & 0 & 1 \times 10^{10} & 0 & 0 \\ 0 & 0 & 0 & 0 & 5 \times 10^9 & 0 \\ 0 & 0 & 0 & 0 & 0 & 1 \times 0^9 \end{bmatrix} \quad (3)$$

In each part of this section, the effects of base isolation system on seismic response of liquid storage tanks for each aspect ratio and earthquake can be seen, and, at the end of each part, there is a Table that shows the summaries.

6. Geometrical specifications of tanks

To carry out the Finite Element Analysis of isolators, the dimensions of tanks are based on the API 650 (Standard 1988) as shown in Table 4 representing the fluid height. The Geometrical properties of baffle, which are shown in Fig. 9, are listed in Table 5 (Cho and Lee 2004). The dimensions of the base-isolated system are illustrated in Table 6 (Das *et al.* 2012).

7. Boundary conditions

7.1 Tank and liquid sloshing

In this study, the effect of base-isolator on the seismic

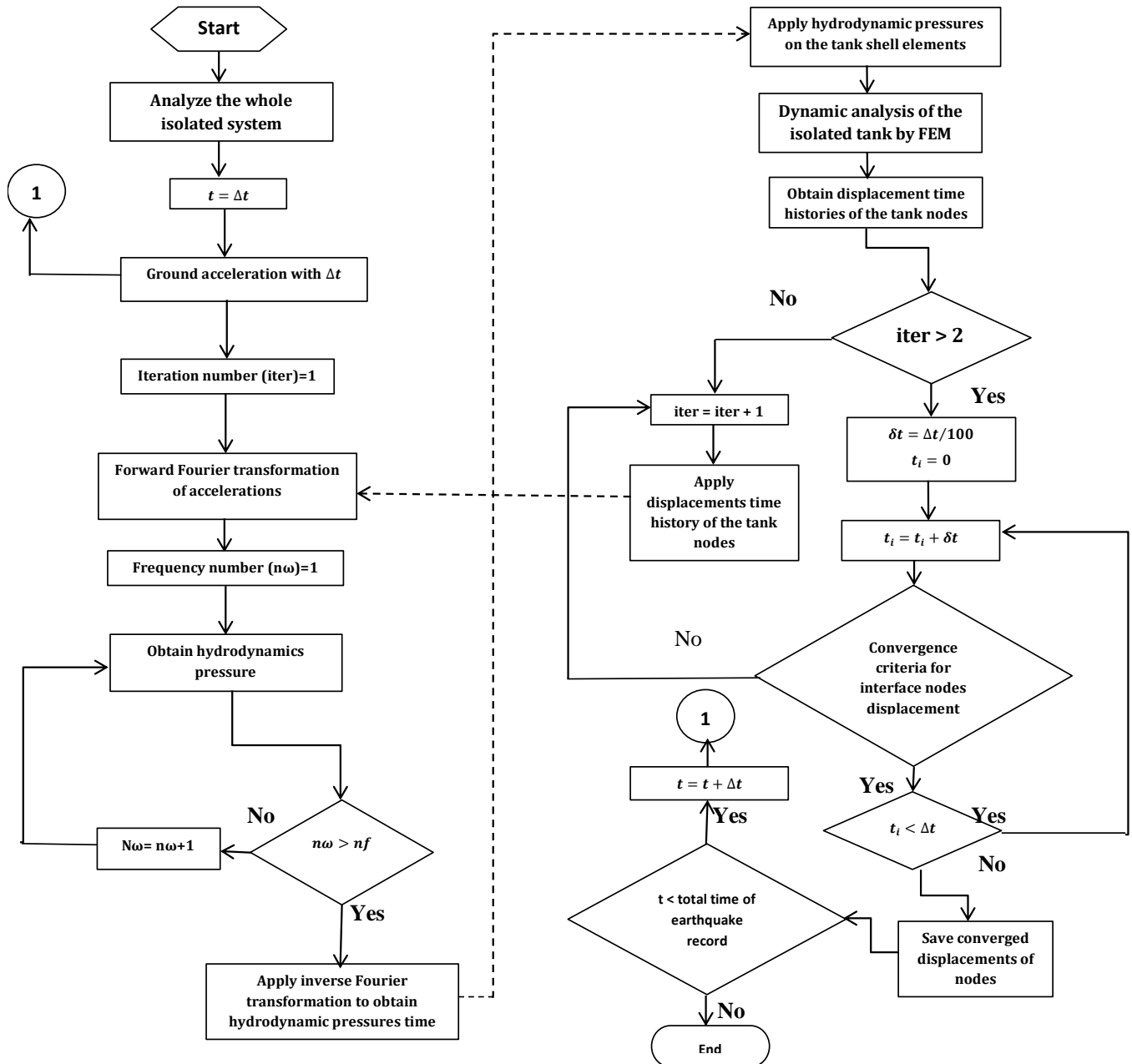


Fig. 8 Flowchart of the simulation with FEM

response of liquid storage tanks, with different aspect ratios under diverse earthquakes, is investigated. Accordingly, three real well-known earthquakes of Iran are selected: Manjil (1990), Tabas (1978), Naghan (1977) (Shekari *et al.* 2010). The Peak Ground Acceleration (PGA) of these earthquake records are 0.8 g, 0.81 g, and 0.84 g (Shekari *et al.* 2010).

The seismic isolation subsystem is shown in Fig. 10a. The contained liquid is considered incompressible, inviscid, and has no rotational motion. Therefore, the governing equation of liquid motion is expressed by the recognized Laplace differential equation.

$$\nabla^2 \varphi = 0 \quad (4)$$

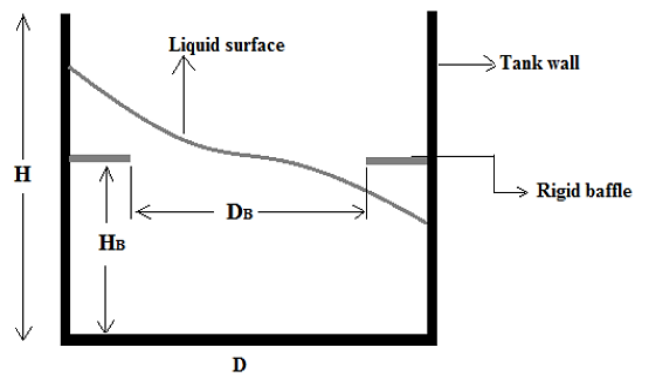


Fig. 9 The position of baffles on the tank body

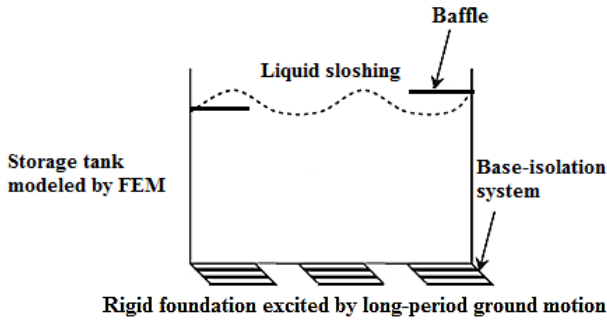


Fig. 10(a) Model of a liquid storage tank on the base-isolation system

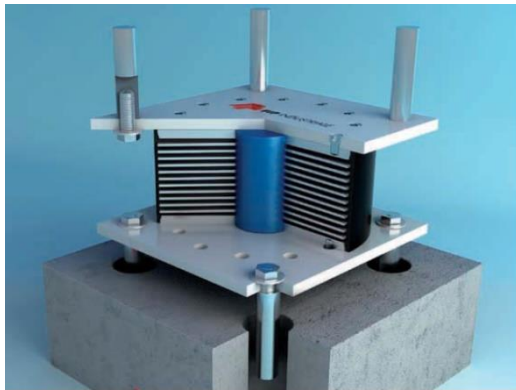


Fig. 10(b) Connection between isolation units and tank bottom (Yen and Lee 2000)



Fig. 10(c) installation of isolation units (Kawamura *et al.* 2000)

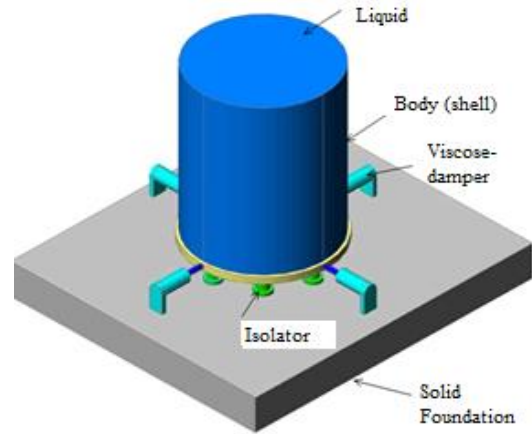


Fig. 10(d) Connection between isolation units and solid foundation

Kinematic and dynamic boundary conditions are linearized for the free surface of the contained liquid, and they are considered as follows (Shekari *et al.* 2010)

$$\frac{\partial \varphi}{\partial z} = \frac{\partial \eta}{\partial t} \quad (5)$$

$$\frac{\partial \varphi}{\partial t} + g\eta = 0 \quad (6)$$

Where φ is the potential velocity function, z is the vertical Cartesian coordinate axis, η is the sloshing height at the free surface of liquid ($z=0$), g is the gravitational acceleration, and t is the time. Further, the boundary condition at the fluid-structure interface is as follows

$$\frac{\partial \varphi}{\partial n} = v_n \quad (7)$$

where v_n is the relative normal fluid velocity at the tank wall, and n indicates the outer normal direction. Using the linearized Bernoulli equation, the hydrodynamic pressure applying to the tank wall is achieved through (Shekari *et al.* 2010)

$$P = -\rho \frac{\partial \varphi}{\partial t} \quad (8)$$

Moreover, the hydrodynamic pressure at the liquid free surface can be obtained by Shekari *et al.* (2010)

$$P = \rho g \eta \quad (9)$$

in which ρ represents the mass density of the liquid. It can be noted that the elastic behaviour of wall is considered; meaning the effect of deformation in the walls on the sloshing of the fluid is ignored.

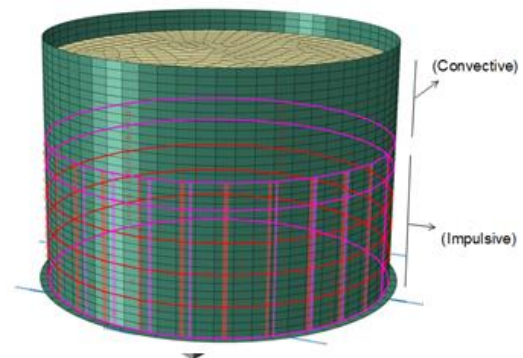


Fig. 10(e) Impulsive and convective high in a medium tank

Based on tank geometries different conditions are utilized. The interested reader can be referred to works by Manos and Clough (1982) for more information on the various parts of a metal liquid storage tank and their significance

7.2 Connection between Isolation units and Tank

The isolation units are in contact with the tank bottom by layers of steels as shown in Fig. 10(b).

As it is shown in Figs. 10(c) and 10(d), at the top isolators, the steel plate connected to concrete slab or ring which is connected at the bottom of the tank. The tank is considered as shell component.

Table 7 Dimension and material properties of fluid and tank

Liquid	ρ (kg/m ³)	h (m)	C_0		
	1000	20	1484		
Tank	ρ (kg/m ³)	E (GPa)	R (m)	H (m)	ν
	7850	207	7.5	22	0.3

Table 8 Seismic response of cylindrical fixed base tank under Imperial Valley 1940 earthquake

Parameter	Present study	Reference	Difference
Base shear (MN)	19.8	21.8	10.1%
Sloshing (m)	0.71	0.63	11.1%

The bottom of the tank is fixed to the rigid slab or rigid plate. Rigid slab with isolators are also connected to the foundation as simply supported.

The tank is modeled by using element S4R with four nodes by having six degree of freedom for each node. The liquid as shown Fig. 10(d) is modeled by element C3D8R with eight nodes. Based on tank height, the liquid behaviour can be considered as impulse and convective. As shown in Fig. 10(e), the tie connection is used to tie convection area to impulsive area. The contact between fluid and tank body is simulated as friction less and also tangential behaviour is employed.

8. Verification of simulation

8.1 Fixed-base tank

To validate the accuracy of the simulation for the application of fluid-structure interaction analysis, the seismic response of cylindrical fixed-base liquid storage tank is achieved and compared with ref (Shekari *et al.* 2010). The required information pertaining to liquid and tank is given in Table 7.

That C_0 is the reference sound speed with the units of m/s.

To access the verification of the results, the seismic response for foregoing tank is achieved under 1940 Imperial Valley with the PGA of 0.235 g. The summary of the maximum seismic response of the foregoing tank is as follows: A good agreement has been shown between the calculated results from the present study and ref (Shekari *et al.* 2010), Table 8.

8.2 Base-isolated tank

The seismic response of base-isolated storage tank under the 1940 Imperial Valley (El Centro) earthquake has been considered. Isolation system properties, such as yield force $F_y=69000$ KN, elastic stiffness= 1.0×10^5 KN/m, and post-Elastic $K_p=0.15 \times 10^5$ KN/m are defined respectively. The above information has been used to validate the results of the present study. The time history of liquid sloshing height of the present study as well as ref¹ is shown in Fig. 11, as it can be seen, the results are in a good agreement.

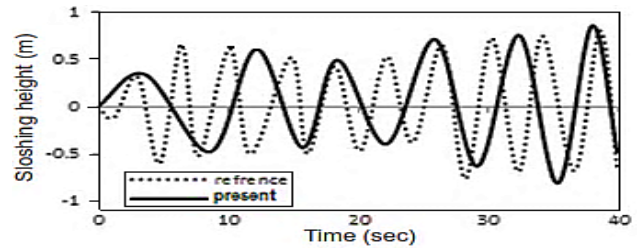


Fig. 11 Liquid sloshing height of the base-isolated tanks

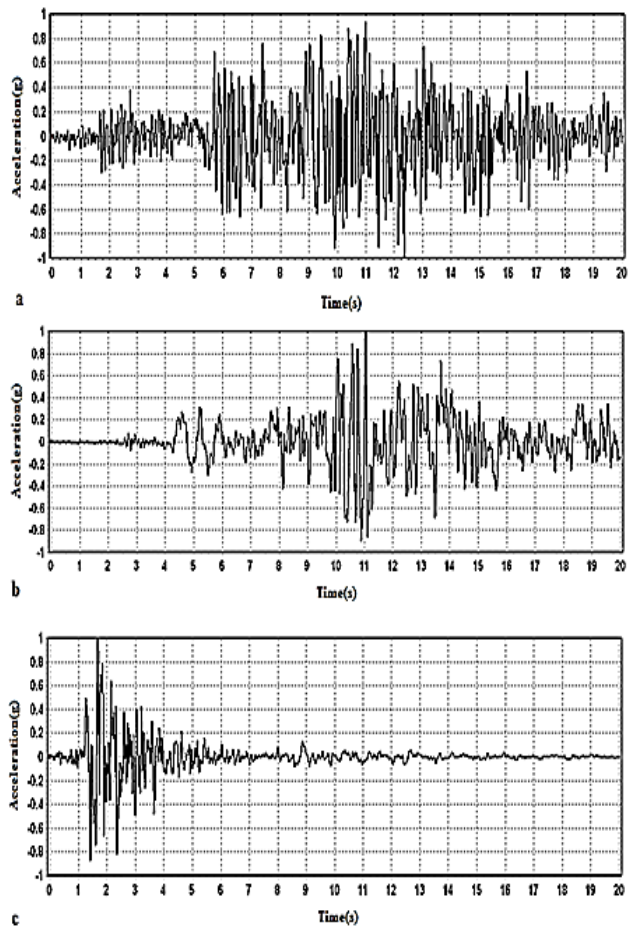


Fig. 12(a) Acceleration time history of earthquakes used in this study: (a) Manjil, (b) Tabas, and (c) Naghan

It is note-worthy that the period of sloshing height obtained from the present study and ref (Shekari *et al.* 2010) are different, while the maximum value of the sloshing height is the same, as shown in Fig. 11. The different periods between two studies can be explained by considering having different time integration methods and numerical simulations.

9. Seismic analysis of base-isolated storage tanks

This section deals with the influence of the base-isolator on the seismic response of liquid storage tanks with different aspect ratios under distinct earthquakes. Accordingly, three real well-known earthquakes of Iran are chosen: Manjil (1990), Tabas (1978), Naghan (1977). It can

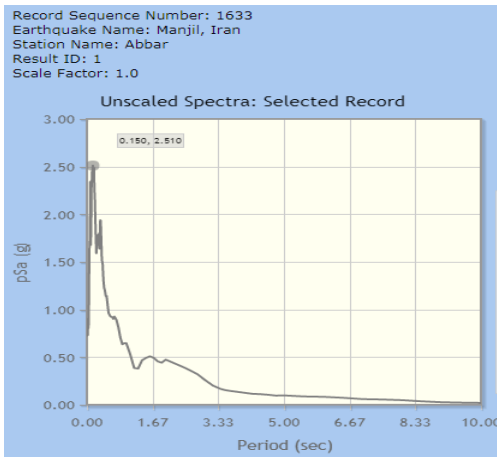


Fig. 12(b) Selected record for acceleration time history of Manjil earthquake

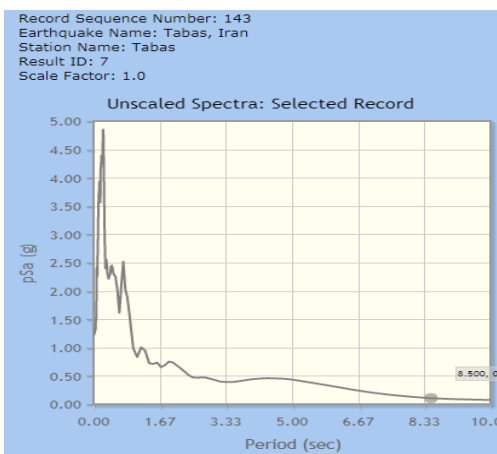


Fig. 12(c) Selected record for acceleration time history of Tabas earthquake

be mentioned that Tabas earthquake is the strongest earthquake in Iran, with a magnitude of 7.8 Richter. The Manjil earthquake had a magnitude of 7.4 Richter which unfortunately made the maximum human injury (by having 35000 dead bodies) in Iran. Naghan earthquake is one of the average earthquakes in Iran with a magnitude of 6 Richter. The reason for selecting the three mentioned grounded motions is that they have varieties of peak ground accelerations as shown in Fig. 12(a). The time history of an earthquake usually indicates the acceleration of Earthquake stimulation during the time of the earthquake. The acceleration time histories of the mentioned earthquakes are shown in Fig. 12(a). In some charts, the speed of displacement of points and in some charts shows displacement of points under earthquake stimulation.

As shown in the Figs. 12(b) and 12(c), in both earthquakes, the maximum acceleration occurs during the low period, and at high period, the earthquake acceleration is moderate.

10. Sloshing height

Sloshing of free surface is indicated by (Senda 1954)

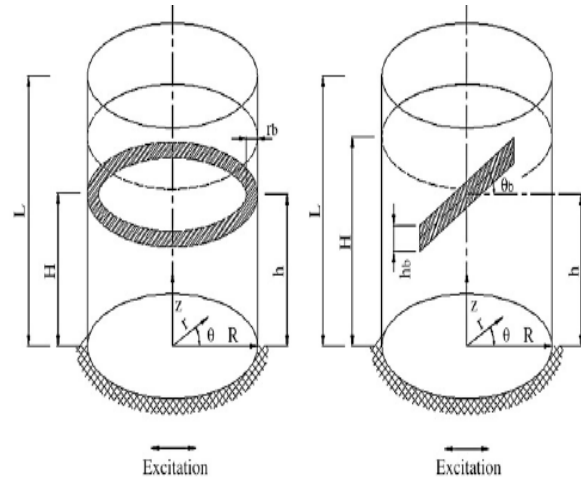


Fig. 13 Tank with baffle ring and vertical baffle (Maleki and Ziyaeifar 2007, Akylidiz *et al.* 2013)

that their assumption is considered in this research.

In this research, natural modes of free oscillations of the sloshing in a cylindrical liquid storage tank with flat bottom are considered. The tank is partially filled with liquid to a height H . The tank wall may be assumed to be rigid with reasonable accuracy because the natural periods of shell vibration modes are much shorter than the natural periods of sloshing modes. The tank is subjected to horizontal ground acceleration in the constant direction. The surface shape will change when the coupling vibration happens to the liquid and the tank, because the liquid sloshing is in the low frequency.

In this research the modal analysis of liquid tanks is not considered. For more information about the modal modeling of nonlinear sloshing can be referred to research by (Ibrahim 2005, Yu, Ma *et al.* 2007, Yan and Yu 2012) and also an analytical solution is investigated by (Matsui 2005, Matsui 2007) to predict the sloshing response of a cylindrical liquid storage tank with a floating roof under seismic excitation.

11. Effect of baffles

As it is expected the baffles are used to damp the forces and make smaller shear force and displacement on supports and foundations. Two type's baffles are common for liquid storage tank as shown in Fig. 21.

The baffles ring and vertical baffles are implemented based on tank's geometry (as shown in Fig. 13). In this study the ring baffles are implemented. The material property of used baffle is: SA-285C with Young modulus=2064 MPa, Poisson ratio=0.3 and density=7840 kh/m^3 .

The baffle is modeled by using element S4R with four nodes by having six degree of freedom for each node. Based on tank height, the liquid behaviour can be considered as impulse and convective. The contact between fluid and baffle is simulated as friction less and also tangential behaviour is employed. The element FLUID 79 is implemented to model fluid domain by having in-plane

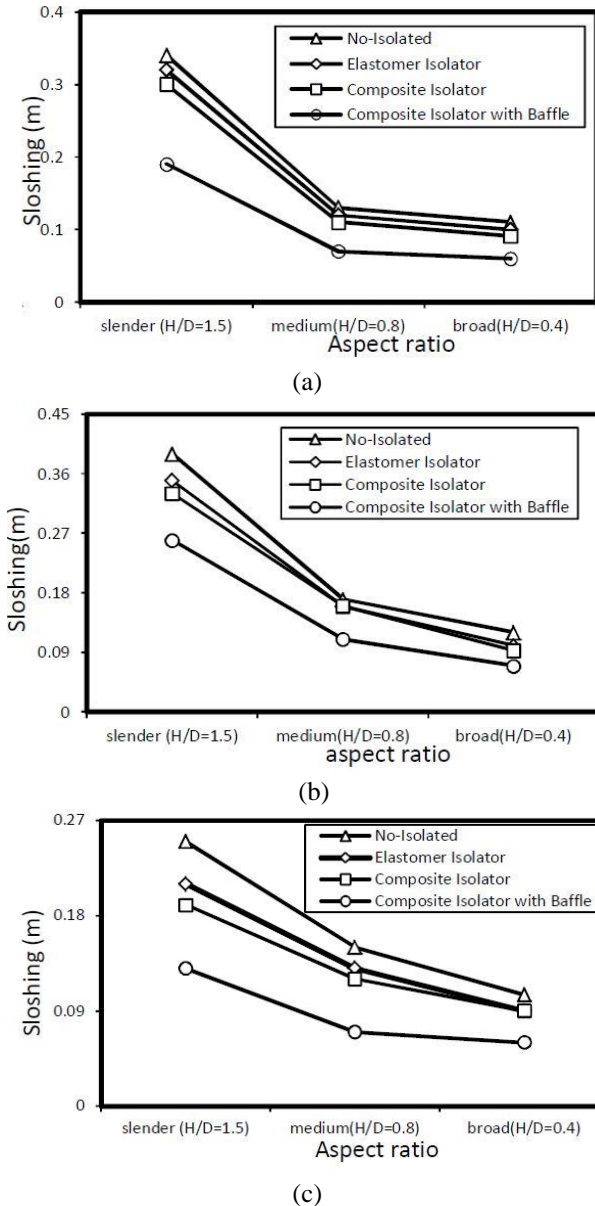


Fig. 14 The maximum liquid sloshing height for various aspect ratios with different base-isolators under (a) Manjil, (b) Tabas, and (c) Naghan earthquakes

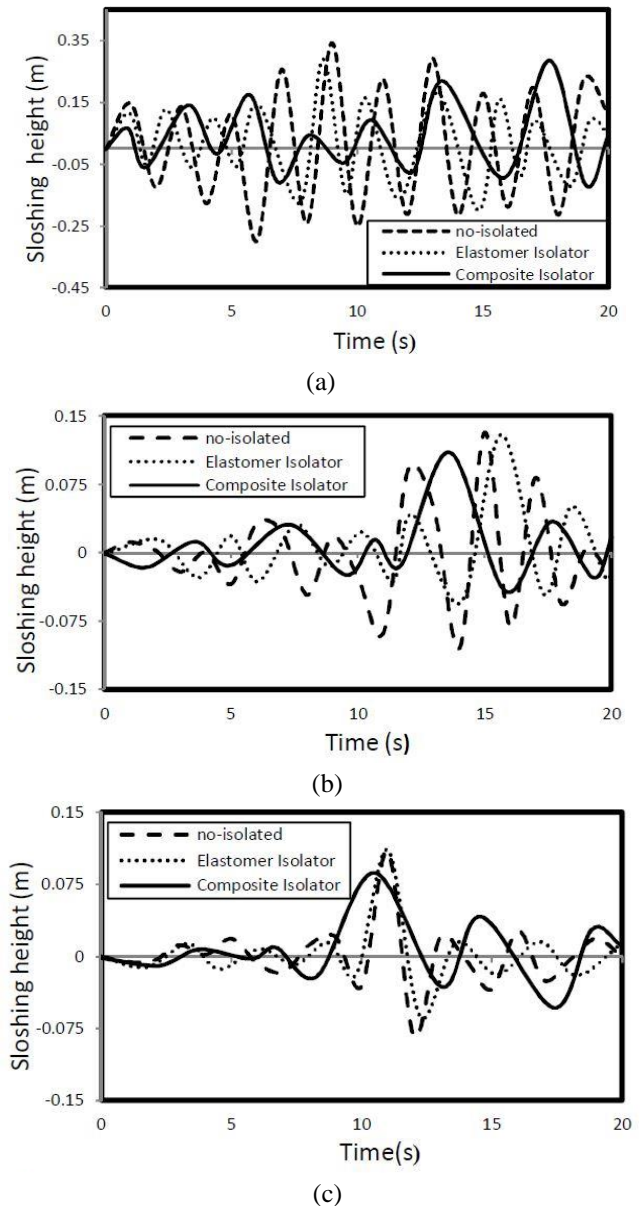


Fig. 15 The time history of maximum liquid sloshing height under Manjil (1988) with different base-isolators for (a) slender tank, (b) medium tank, and (c) broad tank

displacement degree of freedom at each node.

The baffles can make the natural frequencies down; in the mean time they can make the gap between the low frequency coupling system and the high one bigger, which is useful for anti-sloshing.

The maximum liquid sloshing height for the different aspect ratios and diverse base-isolators subjected to three base-excitations is shown in Fig. 14. The time history of Liquid sloshing height for various aspect ratios, and different base-isolators under three distinct earthquakes is shown in Figs. 15-17. To reduce the height of sloshing, baffles, as one of the effective ways, can be installed on the shell of tanks.

According to Table 9, the maximum sloshing height in slender, medium, and broad tanks, under Manjil earthquake, decreases by 6%, 7% and 9% for the elastomer isolated

tanks; 9%, 12% and 10% for the composite isolated tank; and 44%, 46%, 45% for the isolated tanks with baffle. The maximum sloshing height in slender, medium, and broad tanks, under Tabas earthquake, decreases by 12%, 5% and 9% for the elastomer isolated tank; 22%, 24% and 14% for the composite isolated tank; and 33%, 35%, 42% for the isolated tanks with baffle. The maximum sloshing height in slender, medium, and broad tanks, under Naghan earthquake, decreases by 10%, 13% and 16% for the elastomer isolated tank with isolator; 11%, 24% and 22% for the composite isolated tank; and 44%, 53%, 54% for the isolated tanks with baffle.

As described through Figs. 14-17, and in Table 9, the sloshing and displacement increased due to the base-isolation system, but it is not considerable. One of the reasons for the low increase, or decrease in sloshing is that s

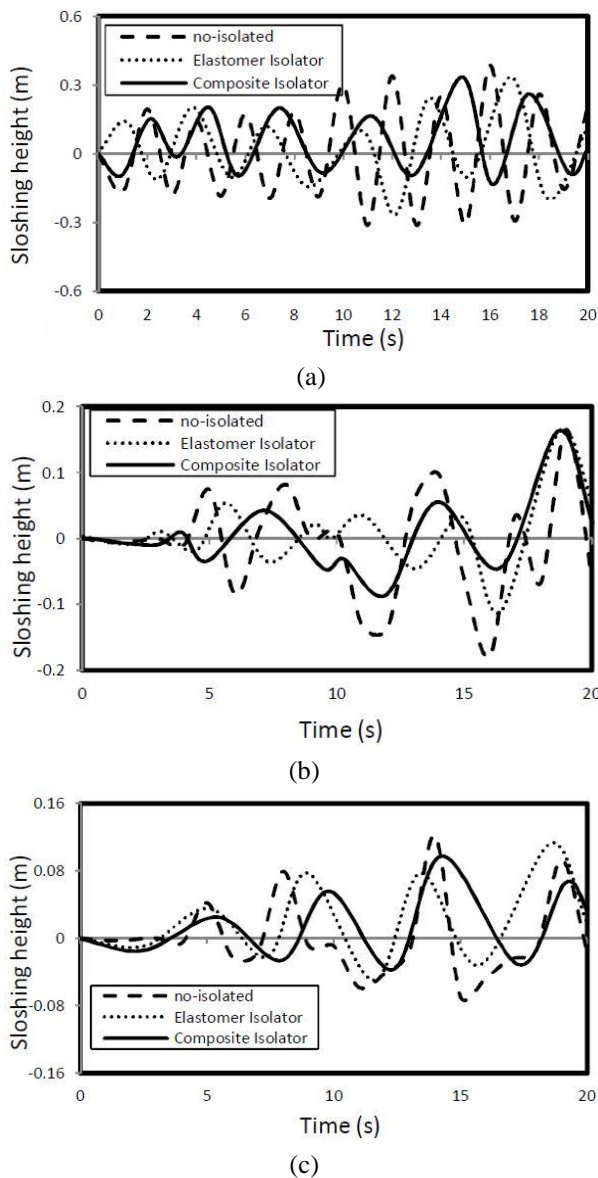


Fig. 16 The time history of maximum radial displacement of tank wall under Tabas (1978) with different base-isolators for (a) slender tank, (b) medium tank, and (c) broad tank

the sloshing height depends on base excitation, and the variety in base isolator does not have any effects on the sloshing height, but the composite isolator can just control this sloshing in a limited area. While using baffle and composite isolator, a maximum reduction of sloshing occurred. Because of both, the effect of using baffle is admirable.

According to the Figs. 14-17, and Table 9, the sloshing height in the storage tank is related to the geometry of the tank, so that by decreasing the tank aspect ratio, the sloshing height will be decreased. It has also been reduced by increasing the flexibility. The composite isolators are more advantageous due to their higher flexibility, strength, and energy absorption than other isolators. This feature refers to the use of carbon fiber and elastomer which exist in them. Because of the above-mentioned reasons, the

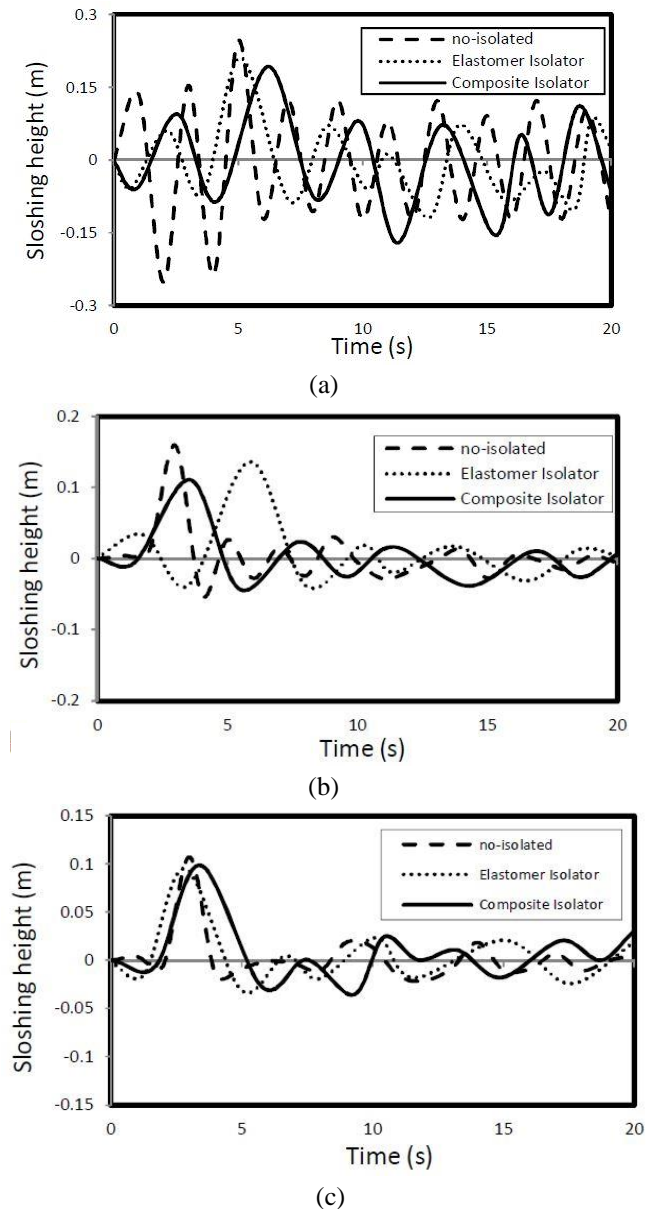


Fig. 17 The time history of maximum liquid sloshing height under Naghan (1977) with different base-isolators for (a) slender tank, (b) medium tank, and (c) broad tank

composite base isolator can reduce sloshing and radial displacement significantly. Likewise, baffles can be applied for the sloshing height control. In the case of the baffle with a composite base isolator, the impressive impact has been seen in reducing the sloshing height due to its geometry in the results.

12. Tank wall radial displacements

As shown in Fig. 18(a), in the case of the tank without isolator, the maximum radial displacements occur close to top surface of the tank wall which is effect of the wall thickness. The composite isolators can controlled the motion of the tank wall in any direction and significantly reduced the interval of the radial displacement. It can be

Table 9 The maximum seismic liquid sloshing height under various ground motions for different aspect ratios

Earthquake	Base type	Maximum Liquid sloshing height (cm)		
		slender	medium	broad
Manjil (1988)	no isolator	0.34	0.13	0.11
	Elastomer isolator	0.32	0.13	0.1
	Composite isolator	0.3	0.11	0.1
	Composite isolator with Baffle	0.19	0.07	0.06
Tabas (1978)	no isolator	0.39	0.17	0.12
	Elastomer isolator	0.35	0.16	0.1
	Composite isolator	0.33	0.16	0.1
	Composite isolator with Baffle	0.26	0.11	0.07
Naghan (1977)	no isolator	0.25	0.15	0.11
	Elastomer isolator	0.21	0.13	0.1
	Composite isolator	0.19	0.12	0.1
	Composite isolator with Baffle	0.14	0.07	0.05

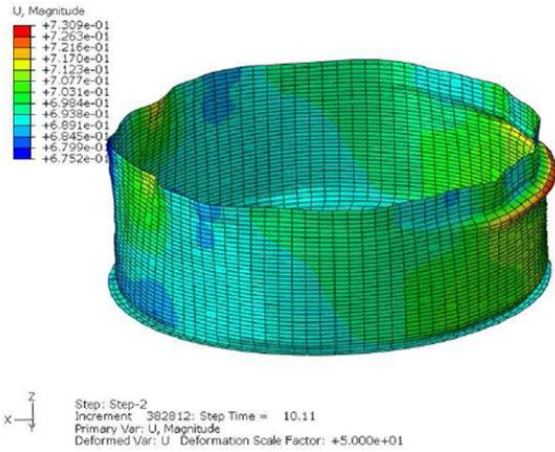


Fig. 18(a) Radial displacement of the tank wall without isolator

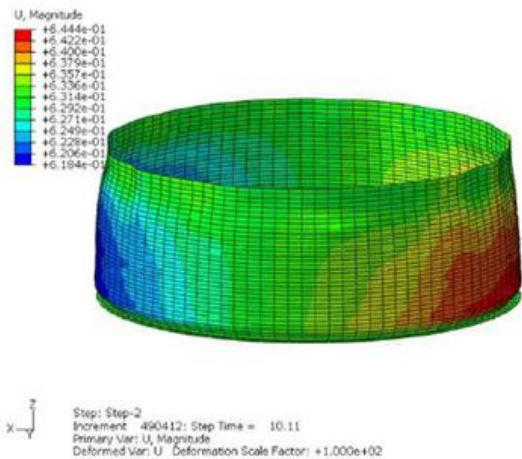


Fig. 18(b) Radial displacement of the tank wall with isolator

noted that in the case of tank with isolator the maximum radial displacements occur close to bottom surface of the tank wall (Fig. 18(b)).

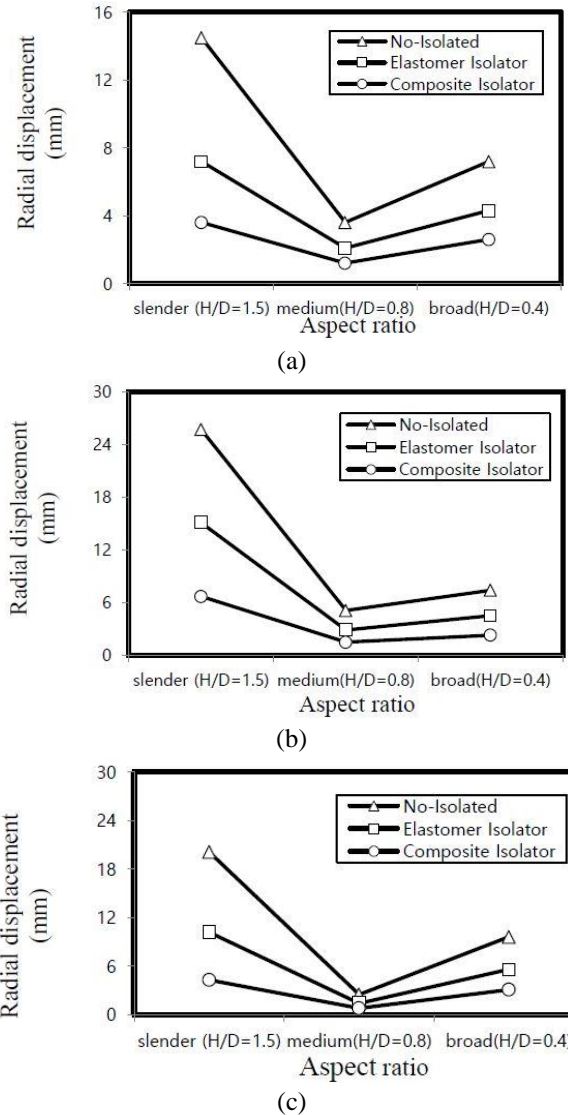


Fig. 19 The tank wall maximum radial displacement for various aspect ratios with different base-isolators under (a) Manjil, (b) Tabas, and (c) Naghan

The maximum tank wall radial displacement for various aspect ratios with different base-isolators, under three distinct earthquakes, is shown in Fig. 19; furthermore, the time history of maximum tank wall radial displacement for various base-isolators with different aspect ratios is shown in Figs. 20-22. According to Table 10, the maximum tank wall radial displacement in slender, medium, and broad tanks, under the Manjil earthquake, decreased by 50%, 46% and 40% for the elastomer isolated tank, and 75%, 66% and 63% for the composite isolated tanks.

The maximum tank wall radial displacement in slender, medium, and broad tanks, under the Tabas earthquake, decreased by 42%, 41% and 38% for the elastomer isolated tanks, and 73%, 70% and 68% for the composite isolated tanks. The maximum tank wall radial displacement in slender, medium, and broad tanks, under the Naghan earthquake, decreased by 50%, 44% and 41% for the elastomer isolated tanks, and 78%, 68% and 67% for the composite isolated tanks.

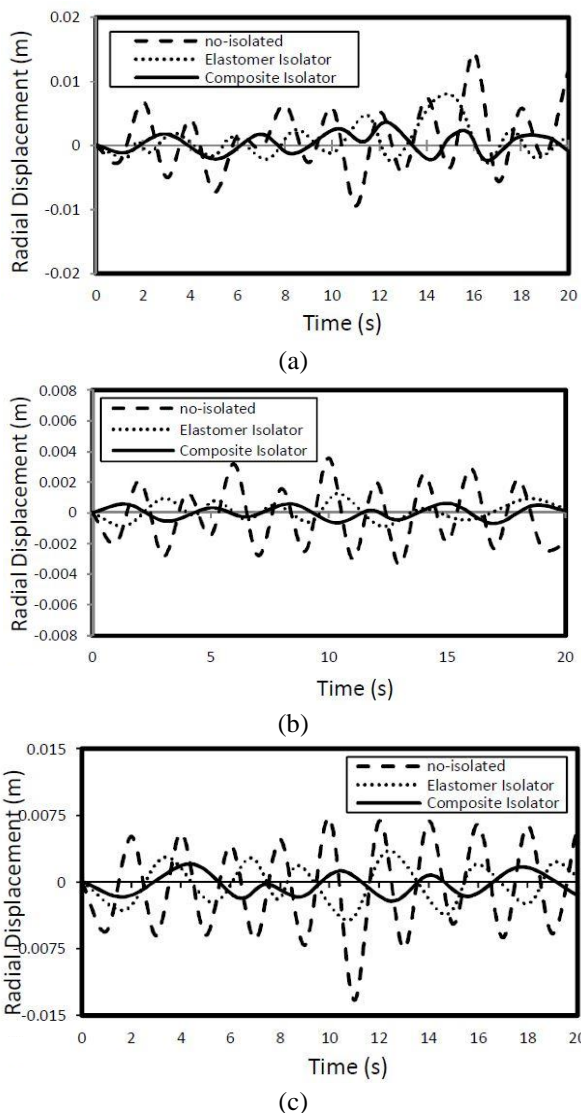


Fig. 20 The time history of maximum radial displacement of tank wall under Manjil (1988) with different base-isolators for (a) slender tank, (b) medium tank, and (c) broad tank

As can be seen from Figs. 19-22, and Table 10, the reason for relatively large increase in radial change in the slender tank by three earthquakes excitation, is the wave height in the tank occurred. Although it was expected for the reduction in the aspect ratio of tanks to lead to reduction in the radial displacement, an optimum aspect ratio for the maximum radial displacement was obtained, as shown in Figs. 19-22 and Table 10. Thus, the range of aspect ratios for medium tanks lies within a reasonable and optimum range.

The maximum reduction of radial displacement occurred, due to the base isolators in slender tanks. But maximum forces act upon slender tanks when compared with medium or broad tanks. It can be concluded that we can select medium tanks as the best aspect ratio. That is, the effect of the base isolators on the radial displacement of the tank wall will be considerable when the flexibility of the tank wall is taken into account.

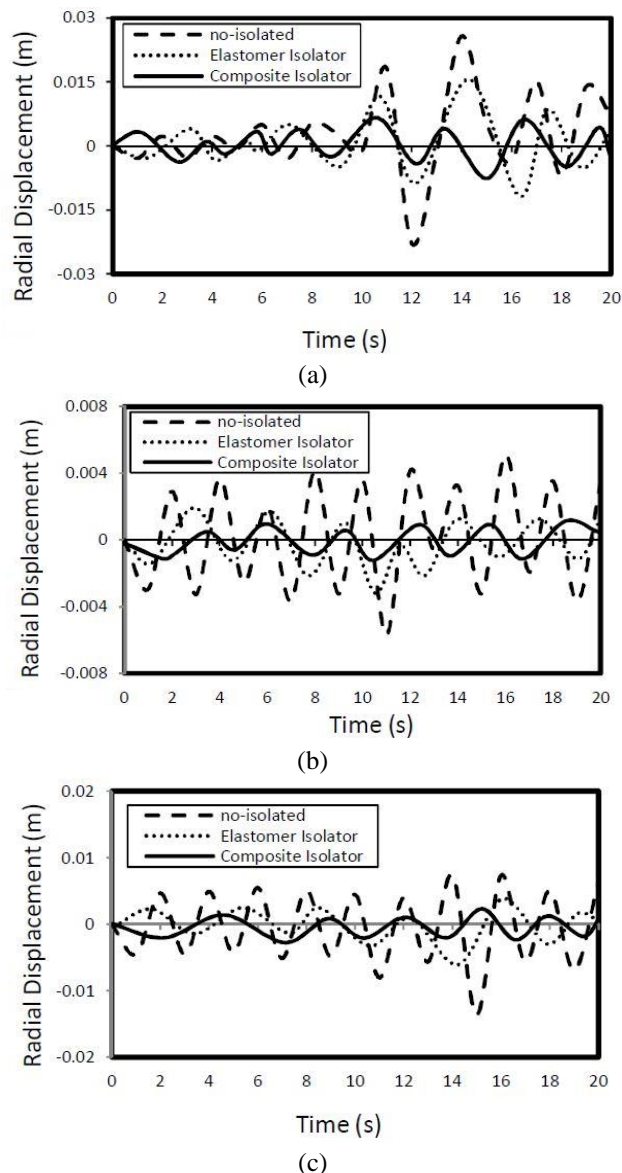


Fig. 21 The time history of maximum radial displacement of tank wall under Tabas (1978) with different base-isolators for (a) slender tank, (b) medium tank, and (c) broad tank

Table 10 The maximum radial displacement under various ground motions for different aspect ratios

Earthquakes	Type of Isolator	Radial Displacement (mm)		
		Slender	Medium	broad
Manjil (1988)	No-Isolated	14.5	3.6	7.2
	Elastomer Isolator	7.2	2.1	4.3
	Composite Isolator	3.6	1.2	2.6
Tabas (1978)	No-Isolated	25.7	5.1	7.41
	Elastomer Isolator	15.1	2.9	4.51
	Composite Isolator	6.7	1.5	2.3
Naghan (1977)	No-Isolated	20.1	2.5	9.6
	Elastomer Isolator	10.2	1.4	5.6
	Composite Isolator	4.3	0.8	3.1

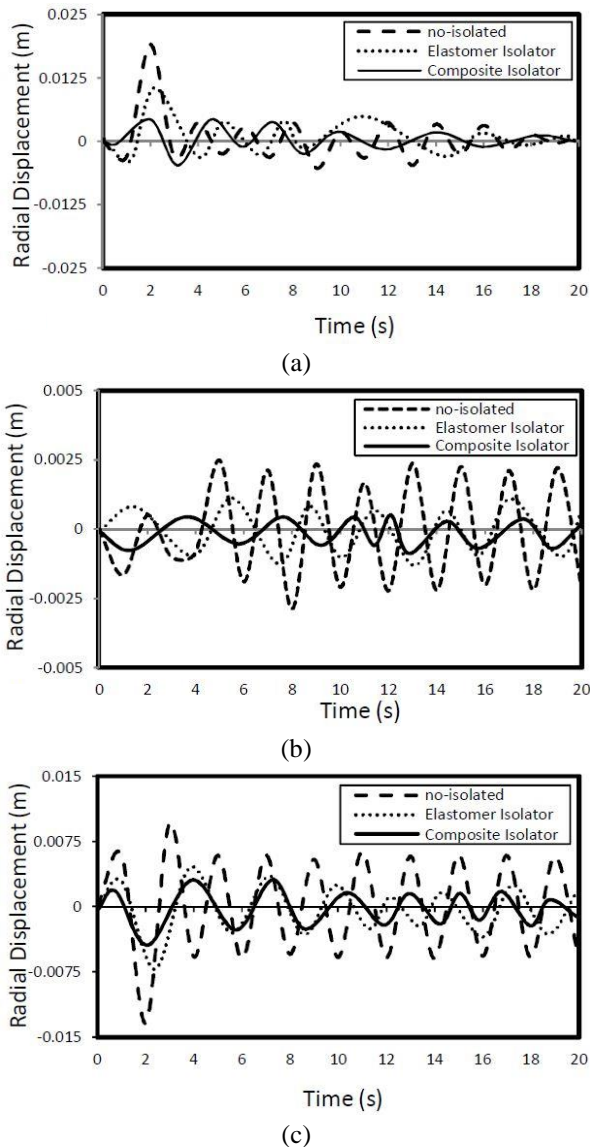


Fig. 22 The time history of maximum radial displacement of tank wall under Naghan (1977) with different base-isolators for (a) slender tank, (b) medium tank, and (c) broad tank

13. Conclusions

The seismic conditions for storage tanks, which are located in high-risk zones of Iran, have been focused in this research, using the composite elastomeric as a part of a base isolator.

The liquid storage tanks, with different materials and various aspect ratios (height to radius), are isolated from base. The important parameters that affect the seismic response of these tanks, such as aspect ratios (height to radius), the flexibility of base isolators, the radial displacement of tank walls, and the sloshing height, have been studied and compared together. This work describes the development of a new device for the seismic isolation of structures. A Fiber Reinforced Rubber Bearing with hyper elastic and visco-elastic behavior of elastomer and orthotropic behavior of carbon fiber was investigated in a

wide parametric numerical program by means of the Finite Element analyses. Contact elements were utilized to model the isolator-plate interfaces. This modeling was done using 3-D surface-to-surface contact elements. Several different bearings were investigated in both static and dynamic conditions in order to obtain the full description of their behaviour. Many analyses were performed with a number of layers, geometries, boundary conditions and material constitutive models. It is assumed that the tank wall is elastic, and fluid is incompressible and inviscid. To verify the reliability and robustness of the work, the results of the seismic analysis, considering the tank wall flexibility, are compared with the available solutions in the literature for flexible tanks. Shear base force and maximum stress in the tank walls are the deciding factors in the design of base-isolated liquid storage tanks. The installation of base isolator has a profound impact on these two parameters (stress and shear force); therefore, it will be discussed in detail in Part II.

The most important results of the analysis of seismic response of base isolated liquid storage tanks are:

1. With reduction in the aspect ratio of tanks without isolators, the investigated parameters (sloshing and radial displacements) were reduced significantly, but with base isolators, this reduction is more significant, especially with composite isolators that reduced the parameters to 70%.
2. The sloshing in tanks depends on the horizontal acceleration of earthquakes. Otherwise, more acceleration leads to great sloshing heights. Hence, isolators cannot decrease the sloshing height, but can control it.
3. Baffles can reduce the sloshing height of tanks substantially. They are able to control and improve the liquid displacements; hence, the performance of these devices in tanks cannot be neglected.
4. The flexibility of tank walls influences the radial displacement of tank walls remarkably. In other words, maximum radial displacement decreases considerably.
5. The sloshing height depends on the aspect ratio of tanks. If aspect ratio decreases, sloshing height will also decrease. Moreover, with increase in the flexibility and strength of base isolators, this parameter can be reduced. Composite isolators can further decrease sloshing because of their high strength and flexibility in comparison with other isolators.

Acknowledgments

The research described in this paper was financially supported by the Malayer University of Iran.

References

- Abali, E. and Uçkan, E. (2010), "Parametric analysis of liquid storage tanks base isolated by curved surface sliding bearings", *Soil Dyn. Earthq. Eng.*, **30**(1), 21-31.
- ABAQUS, ABAQUS Inc..
- Akyildiz, H., Ünal, N.E. and Aksoy, H. (2013), "An experimental

- investigation of the effects of the ring baffles on liquid sloshing in a rigid cylindrical tank”, *Ocean Eng.*, **59**, 190-197.
- Andrade, L. and Tuxworth, J. (2009), “Seismic protection of structures with modern base isolation technologies”, Paper 7a-3, Concrete Solutions.
- Bagheri, S., Rofooei, F. and Bozorgnia, Y. (2005), “Evaluation of the seismic response of liquid storage tanks”, *Proceedings of the Tenth International Conference on Civil, Structural and Environmental Engineering Computing*.
- Carta, G., Movchan, A.B., Argani, L.P. and Bursi, O.S. (2016), “Quasi-periodicity and multi-scale resonators for the reduction of seismic vibrations in fluid-solid systems”, *Int. J. Eng. Sci.*, **109**, 216-239.
- Chen, X., Li, J., Li, Y. and Gu, X. (2016), “Lyapunov-based semi-active control of adaptive base isolation system employing Magnetorheological Elastomer base isolators”, *Earthq. Struct.*, **11**(6), 1077-1099.
- Cho, J. and Lee, H. (2004), “Numerical study on liquid sloshing in baffled tank by nonlinear finite element method”, *Comput. Meth. Appl. Mech. Eng.*, **193**(23), 2581-2598.
- Cho, K.H., Kim, M.K., Lim, Y.M. and Cho, S.Y. (2004), “Seismic response of base-isolated liquid storage tanks considering fluid-structure-soil interaction in time domain”, *Soil Dyn. Earthq. Eng.*, **24**(11), 839-852.
- Das, A., Dutta, A. and Deb, S. (2012), “Modeling of fiber-reinforced elastomeric base isolators”, *15th World Conference on Earthquake Engineering*, Lisbon, Portugal.
- Golzar, F., Shabani, R., Tariverdilo, S. and Rezazadeh, G. (2012), “Sloshing response of floating roofed liquid storage tanks subjected to earthquakes of different types”, *J. Press. Ves. Technol.*, **134**(5), 051801.
- Goudarzi, M.A. (2015), “Seismic design of a double deck floating roof type used for liquid storage tanks”, *J. Press. Ves. Technol.*, **137**(4), 041302.
- Goudarzi, M.A. and Sabbagh-Yazdi, S.R. (2012), “Investigation of nonlinear sloshing effects in seismically excited tanks”, *Soil Dyn. Earthq. Eng.*, **43**, 355-365.
- Hall, J.F., Holmes, W. and Somers, P. (1994), “Northridge earthquake, January 17, 1994”, Preliminary Reconnaissance Report.
- Hanson, R.D. (1973), “Behavior of liquid-storage tanks, the Great Alaska Earthquake of 1964”, *Proceedings of the National Academy of Science*, Washington, **7**, 331-339.
- Housner, G.W. (1963), “The dynamic behavior of water tanks”, *Bull. Seismol. Soc. Am.*, **53**(2), 381-387.
- Ibrahim, R.A. (2005), *Liquid Sloshing Dynamics: Theory and Applications*, Cambridge University Press.
- Jangid, R. and Datta, T. (1995), “Seismic behavior of base-isolated buildings-a state-of-the-art review”.
- Jennings, P. and Housner, G. (1973), “The San Fernando, California, earthquake of February 9, 1971”, *Proceedings of the Fifth*.
- KAmrAvA, A. (2015), “Seismic isolators and their types”, *Curr. World Environ.*, **10**, 27-32.
- Kawamura, S., Sugisaki, R., Ogura, K., Maezawa, S., Tanaka, S. and Yajima, A. (2000), “Seismic isolation retrofit in Japan”, *12th World Conference on Earthquake Engineering*.
- Kelly, J. and Takhirov, S. (2002), “Analytical and experimental study of fiber-reinforced strip isolators. PEER Report 2002/11, Pacific Earthquake Engineering Research Center”, University of California, Berkeley.
- Kelly, J.M. (1986), “Aseismic base isolation: review and bibliography”, *Soil Dyn. Earthq. Eng.*, **5**(4), 202-216.
- Kelly, J.M. and Takhirov, S.M. (2001), “Analytical and experimental study of fiber-reinforced elastomeric isolators”, Pacific Earthquake Engineering Research Center.
- Kim, M.K., Lim, Y.M., Cho, S.Y., Cho, K.H. and Lee, K.W. (2002), “Seismic analysis of base-isolated liquid storage tanks using the BE-FE-BE coupling technique”, *Soil Dyn. Earthq. Eng.*, **22**(9), 1151-1158.
- Kim, N.S. and Lee, D.G. (1995), “Pseudodynamic test for evaluation of seismic performance of base-isolated liquid storage tanks”, *Eng. Struct.*, **17**(3), 198-208.
- Losanno, D., Spizzuoco, M. and Serino, G. (2014), “Optimal design of the seismic protection system for isolated bridges”, *Earthq. Struct.*, **6**, 969-999.
- Luo, H., Zhang, R. and Weng, D. (2016), “Mitigation of liquid sloshing in storage tanks by using a hybrid control method”, *Soil Dyn. Earthq. Eng.*, **90**, 183-195.
- Maleki, A. and Ziyaeifar, M. (2007), “Damping enhancement of seismic isolated cylindrical liquid storage tanks using baffles”, *Eng. Struct.*, **29**(12), 3227-3240.
- Malhotra, P.K. (1997), “New method for seismic isolation of liquid-storage tanks”, *Earthq. Eng. Struct. Dyn.*, **26**(8), 839-847.
- Manos, G. and Talaslidis, D. (1988), “Response of cylindrical tanks subjected to lateral loads-correlation between analytical and experimental results”, *Proceedings of the 9th World Conference on Earthquake Engineering*.
- Manos, G.C. (1986), “Earthquake tank-wall stability of unanchored tanks”, *J. Struct. Eng.*, **112**(8), 1863-1880.
- Manos, G.C. and Clough, R.W. (1985), “Tank damage during the May 1983 Coalinga earthquake”, *Earthq. Eng. Struct. Dyn.*, **13**(4), 449-466.
- Matsui, T. (2005), “Sloshing in a cylindrical liquid storage tank with floating roof under earthquake excitation: Analytical solution”, *Tran. Arch. Inst. JPN, J. Struct. Constr. Eng.*, **594**, 167-173.
- Matsui, T. (2007), “Sloshing in a cylindrical liquid storage tank with a floating roof under seismic excitation”, *J. Press. Ves. Technol.*, **129**(4), 557-566.
- Moon, B.Y., Kang, G.J., Kang, B.S. and Kelly, J.M. (2002), “Design and manufacturing of fiber reinforced elastomeric isolator for seismic isolation”, *J. Mater. Proc. Technol.*, **130**, 145-150.
- Niwa, A. and Clough, R.W. (1982), “Buckling of cylindrical liquid-storage tanks under earthquake loading”, *Earthq. Eng. Struct. Dyn.*, **10**(1), 107-122.
- Ogden, R. (1972), “Large deformation isotropic elasticity-on the correlation of theory and experiment for incompressible rubberlike solids”, *Proceedings of the Royal Society of London A: Mathematical, Physical and Engineering Sciences*, The Royal Society.
- Senda, K. (1954), “On the vibration of an elevated water-tank-I”, *Tech. Rep. Osaka Univ.*, **4**, 247-264.
- Shekari, M., Khaji, N. and Ahmadi, M. (2009), “A coupled BE-FE study for evaluation of seismically isolated cylindrical liquid storage tanks considering fluid-structure interaction”, *J. Fluid. Struct.*, **25**(3), 567-585.
- Shekari, M., Khaji, N. and Ahmadi, M. (2010), “On the seismic behavior of cylindrical base-isolated liquid storage tanks excited by long-period ground motions”, *Soil Dyn. Earthq. Eng.*, **30**(10), 968-980.
- Shrimali, M. and Jangid, R. (2002), “Seismic response of liquid storage tanks isolated by sliding bearings”, *Eng. Struct.*, **24**(7), 909-921.
- Soleimanloo, H.S. and Barkhordari, M.A. (2013), “Effect of shape factor and rubber stiffness of fiber-reinforced elastomeric bearings on the vertical stiffness of isolators”, *Trend. Appl. Sci. Res.*, **8**(1), 14.
- Standard, A.P.I.A.P.I. (1988), *Welded Steel Tanks for Oil Storage*.
- Standard, A.S.T.M. (2008), *Standard Specification for Carbon Structural Steel, A36/A36 M*.
- Steinbrugge, K.V. and Flores, R. (1963), “The Chilean earthquakes of May, 1960: A structural engineering viewpoint”,

- Bull. Seismol. Soc. Am.*, **53**(2), 225-307.
- Tsai, H.C. and Kelly, J.M. (2002), "Stiffness analysis of fiber-reinforced rectangular seismic isolators", *J. Eng. Mech.*, **128**(4), 462-470.
- Veletsos, A. (1974), "Seismic effects in flexible liquid storage tanks", *Proceedings of the 5th World Conference on Earthquake Engineering*.
- Veletsos, A.S. and Auyang, J. (1977), "Earthquake response of liquid storage tanks", *Adv. Civil Eng. Thr. Eng. Mech.*, ASCE, 1-24.
- Wang, Y.P., Teng, M.C. and Chung, K.W. (2001), "Seismic isolation of rigid cylindrical tanks using friction pendulum bearings", *Earthq. Eng. Struct. Dyn.*, **30**(7), 1083-1099.
- Yan, J. and Yu, H.L. (2012), "The free sloshing modal analysis of liquid tank with baffles", *Adv. Mater. Res.*, **347**, 2404-2408.
- Yang, J.Y. (1976). *Dynamic Behavior of Fluid Tank Systems*, Rice University.
- Yen, K.Z. and Lee, Y.J. (2000), *Passive Vibration Isolating System*, Google Patents.
- Yu, Y.S., Ma, X.R. and Wang, B.L. (2007), "Multidimensional modal analysis of liquid nonlinear sloshing in right circular cylindrical tank", *Appl. Math. Mech.*, **28**(8), 1007-1018.
- Yu, Y., Royel, S., Li, J., Li, Y. and Ha, Q. (2016), "Magnetorheological elastomer base isolator for earthquake response mitigation on building structures: modeling and second-order sliding mode control", *Earthq. Struct.*, **11**(6), 943-966.
- Zhang, H., Li, W., Yang, X., Lu, L., Wang, X., Sun, X. and Zhang, Y. (2007), "Development of polyurethane elastomer composite materials by addition of milled fiberglass with coupling agent", *Mater. Lett.*, **61**(6), 1358-1362.